Monatshefte für Chemie - Chemical Monthly (2024) 155:237–243
https://doi.org/10.1007/s00706-024-03175-7

REVIEW

Impedance changes of the Li-ion cell in the course of discharge

Petr Křivík[1]

Received: 3 October 2023 / Accepted: 10 January 2024 / Published online: 5 March 2024

Abstract
The paper deals with the measurement of the cell impedance parameters during discharging of the Li-ion NCR18650B cell. Re (*Z*) and Im (*Z*) of the battery were measured by PEIS method. The results of the impedance changes during discharging and charging were plot to Nyquist diagrams. The important values namely *Rs*, *Rsei*, *Rct*, *Csei*, *Qsei*, *Cdl*, α, and σ were found during discharging of the Li-ion cell with and without using CPE element.

Graphical abstract

Keywords Li-ion cell · Phase angle · Nyquist diagram · ZARC element

Introduction

Lithium ion cells are currently among the common products of a number of renowned companies (SAFT, VARTA, Sony, Duracell, etc.). The charged cell of the usual design has an open circuit voltage of 2.4–3.7 V and its energy density ranges from 80 to 260 Wh/kg. Self-discharge is about 510% of the capacity per month. The cell has a long cycle life and after 500 cycles, the capacity of Li-ion cell decreases by 10–20%. The electrodes of these cells are very thin (around 200 μm) and are made of intercalating compounds (compounds that can accept an atom or molecule into their crystal lattice). The active material of the positive electrode are metal compounds, the most common types of Li-ion batteries include lithium cobalt Oxide ($LiCoO_2$)—LCO (ICR), lithium manganese oxide ($LiMn_2O_4$)—LMO (IMR), lithium nickel manganese cobalt oxide ($LiNiMnCoO_2$)—NMC (INR), lithium iron phosphate ($LiFePO_4$)—LFP, and lithium nickel cobalt aluminum oxide ($LiNiCoAlO_2$)—NCA (NCR). The negative electrode is carbon (graphite). The second possible material for the negative electrode is lithium titanate (Li_2TiO_3)—LTO. These substances must be sufficiently porous. The matrix must very well receive (intercalate) lithium ions and again easily release them. The collectors of the negative electrodes are usually made of copper foil, the positive electrodes are aluminum foil. Active electrode materials are applied to the collectors. The separators are usually made of a very thin porous film made of polyethylene or polypropylene or a microporous polymer film. The electrolyte is a lithium salt ($LiPF_6$, $LiBF_4$, or $LiClO_4$) and an organic solvent (ether, various mixtures of ethylene-, propylene-, dimethyl- or diethyl carbonate, etc.). The liquid electrolyte is conductive for lithium ions, which travel between the electrodes during discharging and charging [1].

The chemical process in the cell consists only in the transport of lithium ions. During charging, positively charged lithium ions travel to the negative electrode, where they are intercalated in the carbon structure. When discharging, the opposite process takes place—lithium ions travel to the positive electrode, where they are intercalated in the positive active material structure. During the discharge, the

✉ Petr Křivík
Petr.Krivik@vut.cz

[1] Department of Electrotechnology, Brno University of Technology, Brno, Czech Republic

impedance of the Li-ion cell is changing, including ohmic resistance R_s, resistance and capacitance of SEI layer (R_{sei}, C_{sei}), charge transfer resistance R_{ct}, double layer capacity C_{dl}, and Warburg impedance Z_w. Electrochemical impedance spectroscopy (EIS) is a suitable method for determining these parameters. This method is suitable for monitoring the impedance of a Li-ion cell over a wide range of frequencies. Results are displayed by the impedance diagrams [2].

The electrochemical impedance of a battery Z is a complex number, frequency-dependent, described either by its real and imaginary parts Re (Z) and Im (Z), or by its modulus $|Z|$ and phase angle φ. Different frequencies reflect different parameters of the Li-ion cell, from ohmic resistance through resistance and capacitance of the SEI layer, charge transfer resistance at the electrodes, diffusion double layer capacity to Warburg impedance related to ion diffusion in the electrolyte and electrode pores. The SEI layer is a passivation layer formed on the surface of the negative electrode materials of lithium-ion batteries [3].

The general shape of the Nyquist diagram of the complex electrochemical impedance of the battery is shown in Fig. 1. This diagram starts at the highest frequencies around 5 kHz below the x-axis, where the circuit inductance and skin effect predominate. At frequencies around 1 kHz, the ohmic resistance of the Rs cell is presented in the range of mΩ, the imaginary part of the impedance is close to zero. The ohmic resistance includes the resistance of the interconnection, the separator, the electrolyte and the both electrodes. The first arc appears at frequencies in the hundreds of Hz. Here, the phenomena in the SEI layer are applied, which represents the resistance and capacity of the SEI layer. The resistance of the SEI layer indicates the size of the first arc. The second arc appears at frequencies in tens of Hz. Here, the charge transfer resistance at the electrodes R_{ct} and the capacitance of the double layer C_{dl} caused by the distribution of the space charge in the electrochemical double layers are presented. The charge transfer resistance indicates the size

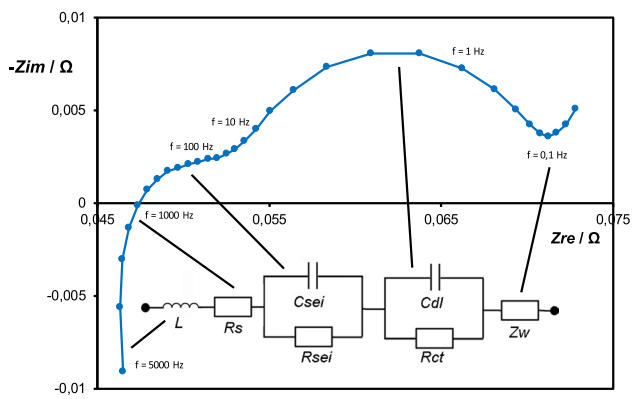

Fig. 1 Nyquist impedance diagram and equivalent Li-ion cell circuit

of the second arc. At the lowest frequencies, the Warburg impedance is presented due to the diffusion of ions in the electrolyte and in the electrodes. All of these parameters can be represented by an equivalent circuit [4].

The cell impedance is:

$$Z = R_S + \frac{R_{sei}}{j\omega C_{sei} R_{sei} + 1} + \frac{R_{ct}}{j\omega C_{dl} R_{ct} + 1} + Z_w, \tag{1}$$

where $Z_w = \frac{\sigma}{\sqrt{\omega}} - j\frac{\sigma}{\sqrt{\omega}}$, $C_{sei}R_{sei} = \tau_{sei}$, and $C_{dl}R_{ct} = \tau_{dl}$.

Zw is the Warburg impedance, σ the Warburg coefficient [$\Omega s^{-1/2}$], and ω the angular frequency [s^{-1}], τ_{sei} is time constant of SEI layer, τ_{dl} time constant of diffuse double layer [s].

From the measured values of the cell impedance at different frequencies, individual parameters of the measured impedance can be found by fitting. When fitting the Nyquist diagram around the middle frequencies corresponding to the SEI layer area, it was shown that the impedance values obtained from the equivalent circuit do not correspond to the measured values and it is necessary to use the constant phase element (CPE) Q, better corresponds to the measured data [5–8]. For a constant phase element, the phase angle of its impedance is independent of frequency and its value is (90°. α). It is caused by the dispersion of capacity caused by inhomogeneities, which result in uneven current and potential distribution. CPE is related to the two-dimensional distribution of frequencies or time constants (due to the surface heterogeneities, non-uniform distribution of charge on the electrode surface) and to the three-dimensional distribution of frequencies or time constants (due to the porosity and roughness of the electrode surface).

The impedance of the CPE element is equal to:

$$Z_{CPE} = \frac{1}{(j\omega)^{\propto} Q_{sei}}, \tag{2}$$

where Q_{SEI} is a type of capacitance with a unit dependent on α [F $s^{\alpha-1}$].

Together with the R_{SEI} resistor of the SEI layer connected in parallel to the CPE, an RQ element, or ZARC element, is created [9]. Its impedance is calculated as:

$$Z_{ARC} = \frac{R_{sei}}{(j\omega)^{\propto} Q_{sei} R_{sei} + 1}. \tag{3}$$

In the Nyquist diagram, the ZARC element creates an arc whose center is for $\alpha < 1$ below the x-axis, see Fig. 2.

The cell impedance with using the ZARC element is:

$$Z = R_S + \frac{R_{sei}}{(j\omega)^{\propto} Q_{sei} R_{sei} + 1} + \frac{R_{ct}}{j\omega C_{dl} R_{ct} + 1} + Z_w. \tag{4}$$

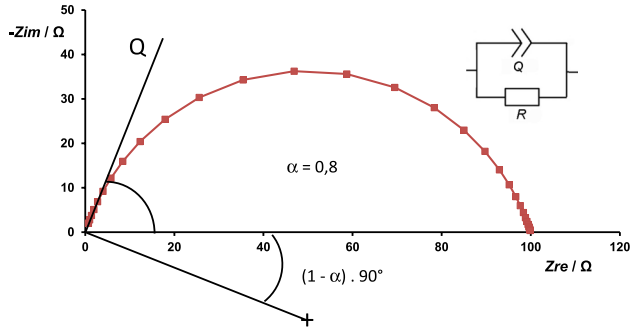

Fig. 2 Geometry of a ZARC element with $\alpha = 0.8$

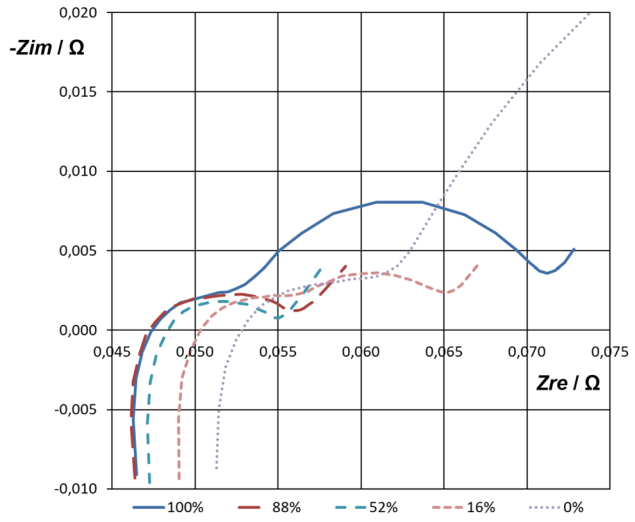

Fig. 3 Nyquist diagram of Li-ion cell during intermittent discharge (SoC = 100–0%)

The aim of this study was to compare the two models that describe the SEI layer, i.e. using the parallel connection of the resistance and capacity of the SEI layer or using the ZARC element—the parallel connection of the resistance and constant phase element Q_{SEI}. From the results of the Nyquist diagram, it is clear that the use of the ZARC element more accurately describes the properties of the SEI layer and the Li-ion cell [9].

Results and discussion

Figure 3 is Nyquist diagram during intermittent discharge of a Li-ion cell. SoC corresponds to a state of charge from 100 to 0%. The measured impedance values were compared with the values obtained from impedance calculations from the cell equivalent circuit. These dependences for a charged cell with an equivalent circuit without CPE and with CPE are shown in Figs. 4 and 5 in the form of Nyquist diagram and in Figs. 6 and 7 in the form of frequency dependence of real and imaginary Z values.

When compare Figs. 4 and 5, or 6 and 7, it is clear that the use of a equivalent circuit with a CPE element gives an impedance curve that corresponds much better to the measured data. Coefficient of determination without CPE element $R^2 = 0.987$, with CPE element $R^2 = 0.997$. The highest difference between the measured and fitted data are for equivalent circuit without a CPE element in the area of medium frequencies (hundreds of Hz), where the influence of the SEI layer is manifested.

The changes in the values of the cell equivalent circuit parameters during discharge without CPE and with CPE are shown in Figs. 8, 9, 10 and 11. DoD (depth of discharge) varies from 100 to 0%.

Fig. 4 Nyquist diagram of a charged Li-ion cell (SoC = 100%) for measured and fitted impedance values without CPE element

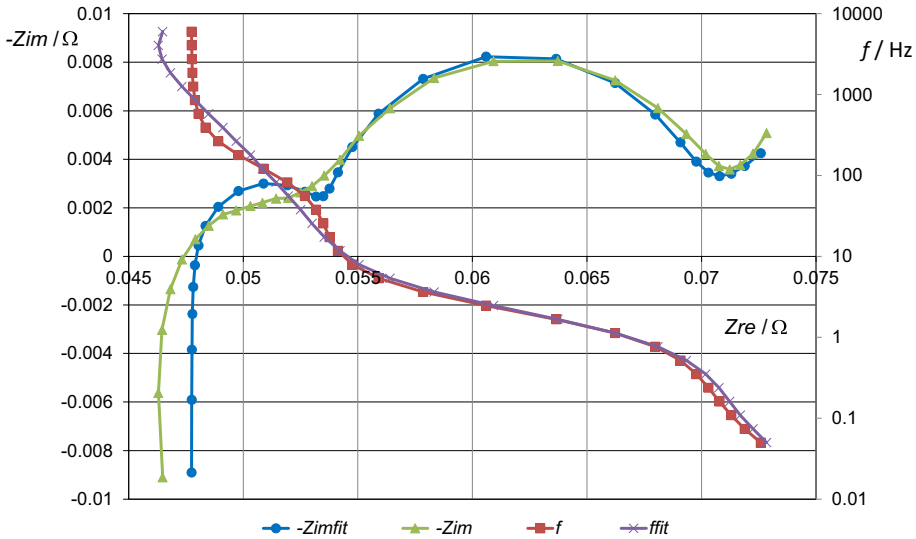

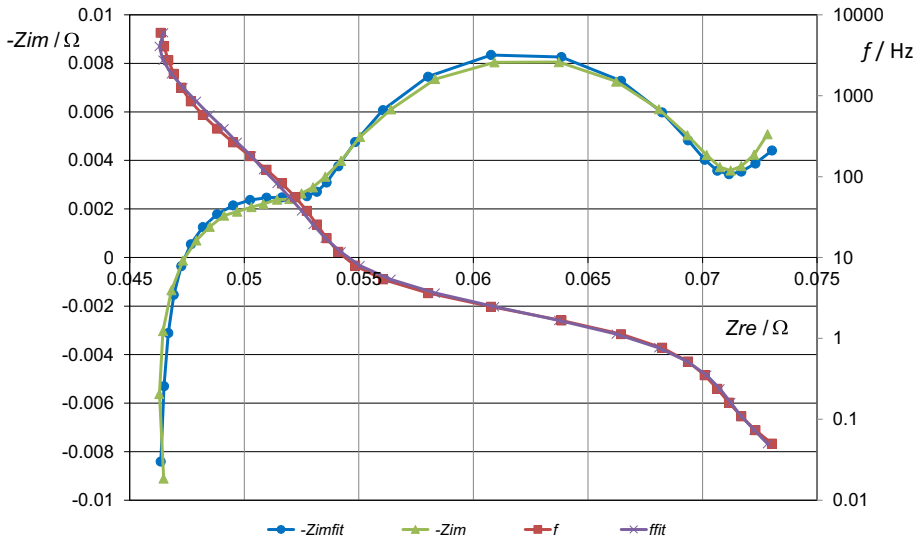

Fig. 5 Nyquist diagram of a charged Li-ion cell (SoC = 100%) for measured and fitted impedance values with CPE element

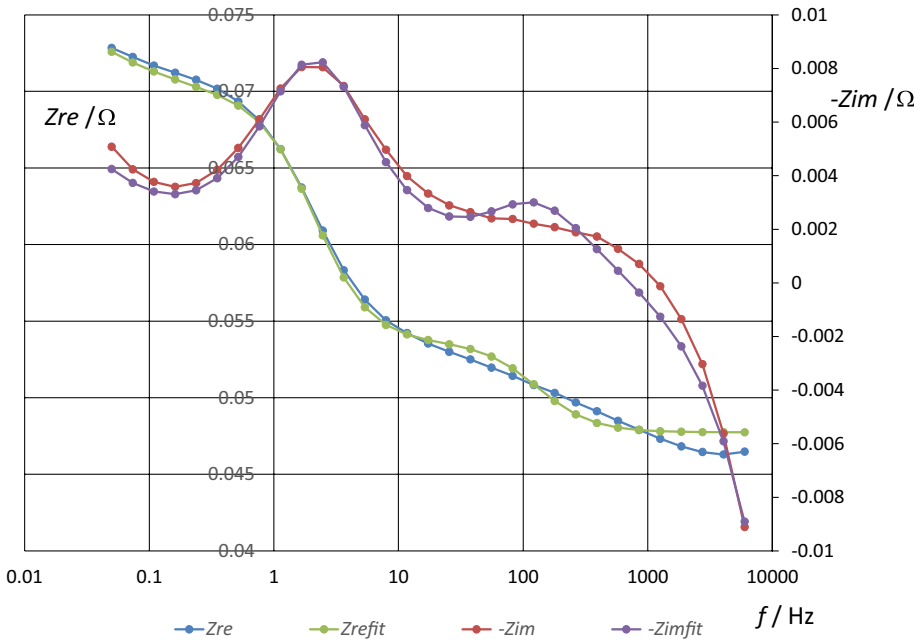

Fig. 6 Frequency dependence of real and imaginary Z values for measured and fitted impedance values without CPE element

It can be seen that the ohmic resistance R_s gradually increases during discharging. This increase is accelerated at the end of discharge. During discharge lithium intercalates into the structure of the positive electrode and increase its resistance. Measured results reveal a drastic change in the electronic conductivity occurring at an early stage of lithium deintercalation (or at the end of lithium intercalation), which may be caused by a transition from polaron to metal. In the case of $LixNiCoAlO_2$ (NCR) or $LixCoO_2$ (LCO) materials, such a transition has been proposed to be responsible for the existence of a two-phase region between the lithium concentrations of $x = 0.95$ and $x = 0.75$, namely, $LixNiCoAlO_2$ or $LixCoO_2$ is a semiconductor for $x > 0.95$ (end of discharge), and is of metallic property for $x < 0.75$ [10].

The charge transfer resistance R_{ct} decreases up to about 50% of DoD during discharging. At the end of the discharge, on the other hand, *Rct* rises sharply. It is obvious that at the end of the discharge, lithium is added to the active mass of the positive electrode and fills the remaining free spaces in the structure of the positive electrode, and this is reflected in the increase of the charge transfer resistance.

The resistance of the SEI layer, R_{sei}, does not change much during discharge, its magnitude is about 0.05 Ω for an equivalent circuit without CPE, comparable to the value

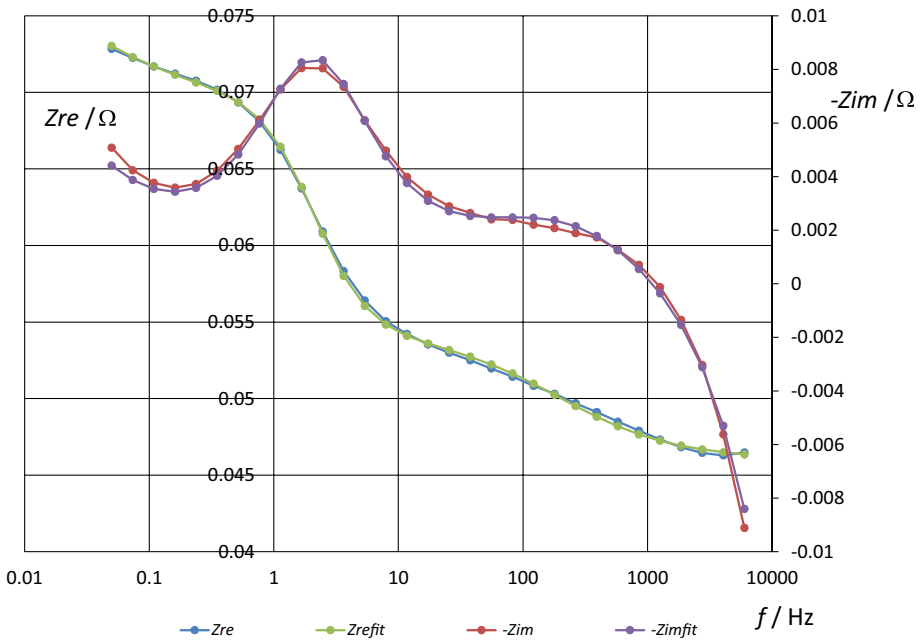

Fig. 7 Frequency dependence of real and imaginary *Z* values for measured and fitted impedance values with CPE element

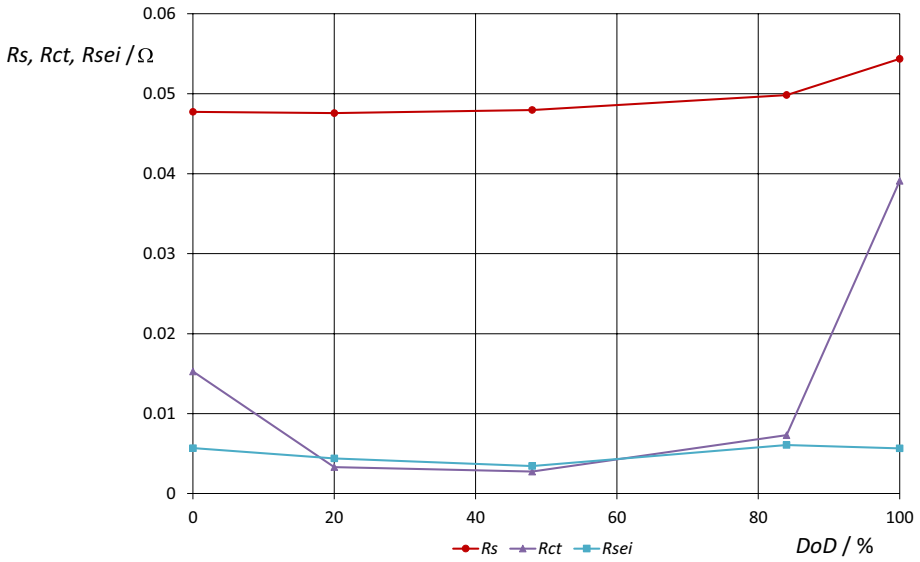

Fig. 8 The dependence of *Rs*, *Rct*, and *Rsei* of the battery during intermittent discharge without CPE (DoD = 0–100%)

of R_{ct} between 20 and 80% of discharge. For a equivalent circuit with CPE, the size of R_{sei} is higher, around 0.09 Ω.

The course of capacities differs for both equivalent circuits. When using a equivalent circuit without CPE, the capacity of the double layer C_{dl} during discharging decreases up to about 50% DoD and at the end of discharge C_{dl} increases sharply.

The capacity of the SEI layer, C_{sei}, has a similar course as the capacity of the C_{dl} double layer. Compared to C_{dl}, it is much lower by 1 to 2 orders of magnitude. When using equivalent circuit with CPE, the capacity of the double layer C_{dl} increases during discharge. Its size is comparable to the capacity of a double layer C_{dl} from equivalent circuit without CPE.

The course and size of the Q_{sei} from equivalent circuit with CPE differs from the C_{sei} from equivalent circuit without CPE. After an initial sharp decrease, Q_{sei} increases slightly during discharge. The size of Q_{sei} is four times higher than C_{sei}. The value of the parameter α is around 0.7.

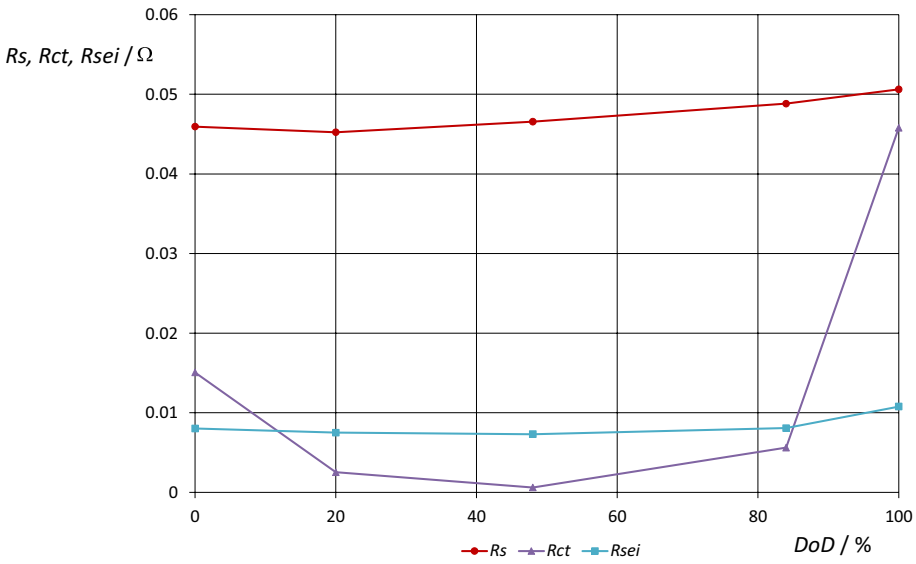

Fig. 9 The dependence of *Rs*, *Rct*, and *Rsei* of the battery during intermittent discharge with CPE (DoD = 0–100%)

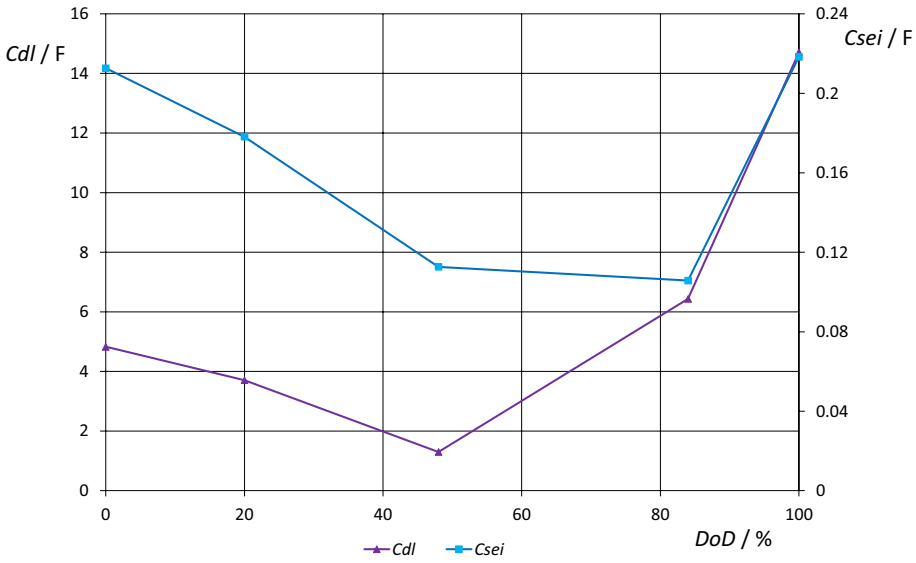

Fig. 10 The dependence of *Cdl* and *Csei* of the battery during intermittent discharge without CPE (DoD = 0–100%)

Conclusion

Nyquist diagrams of the Li-ion cell during discharge were measured. Important parameters of the battery equivalent circuit were found from the diagrams. These parameters indicate the changes of the impedance of the Li-ion cell in different states of discharge. The use of CPE element in the cell equivalent circuit increased the accuracy of the regression function parameter estimation.

Experimental

A Li-ion cell NCR18650B with a nominal capacity of 3350 mAh, a nominal voltage of 3.6 V, an energy density: 676 Wh/l, 243 Wh/kg was used to measure the impedance changes. The positive electrode is composed of $LiNiCoAlO_2$, the negative electrode of graphite, electrolyte: ethylene carbonate, diethyl carbonate, salt: lithium hexafluorophosphate. The cell was placed in a temperature chamber with a temperature of 34.4 °C and subjected to

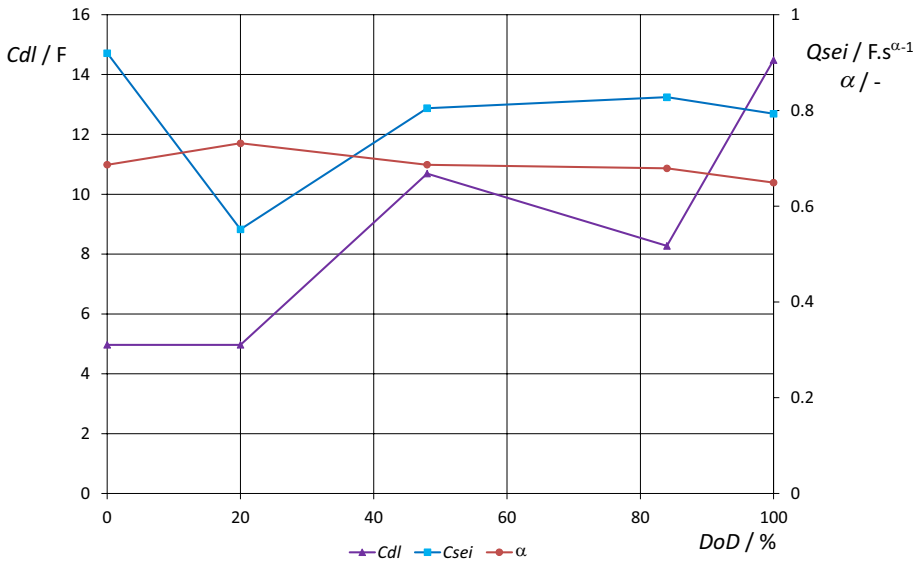

Fig. 11 The dependence of *Cdl* and *Qsei* of the battery during intermittent discharge with CPE (DoD = 0–100%)

intermittent discharging with a current of 0.4 A for 1 h, followed by current off period for 2 h. The measured discharged capacity was 3314 mAh. The voltage limitation at the end of discharging was 2.5 V. Impedance changes were measured by EIS during the experiment. The voltage amplitude at EIS was set at 5 mV, frequency from 6 kHz to 50 mHz, 6 measurements per decade.

Acknowledgements This research work has been supported by the specific research of the Brno University of Technology No. FEKT-S-23-8286.

Funding Open access publishing supported by the National Technical Library in Prague.

Data availability Data is available on request.

References

1. https://batteryuniversity.com/article/bu-205-types-of-lithium-ion (2019)
2. Pérez A, Benavides M, Rozas H, Seria S, Orchard M (2018) Int J Prognostics Health Manage 9:2746
3. Westerhoff U, Kurbach K, Lienesch F, Kurrat M (2016) Energy Technol 4:1620
4. Bao Y, Chen Y (2021) Energies 14:4396
5. Jorcin JB, Orazem M, Pébère N, Tribollet B (2006) Electrochim Acta 51:1473
6. Macdonald D, Urquidi-Macdonald M (1990) J Electrochem Soc 137:515
7. Cole K, Cole R (1941) J Chem Phys 9:341
8. Hampson NA, Karunathilaka SAGR, Leek R (1980) J Appl Electrochem 10:3
9. Heil T, Jossen A (2021) Meas Sci Technol 32:104011
10. Qiu X-Y, Zhuang Q-C, Zhang Q-Q, Cao R, Ying P-Z, Qiang Y-H, Sun S-G (2012) Phys Chem Chem Phys 14:2617